Applied Geochemistry 63 (2015) 70–82

Contents lists available at ScienceDirect

Applied Geochemistry

journal homepage: www.elsevier.com/locate/apgeochem

Sulfate reducing bioreactor dependence on organic substrates for remediation of coal-generated acid mine drainage: Field experiments

Liliana Lefticariu [a, c, *], Evan R. Walters [a], Charles W. Pugh [b], Kelly S. Bender [b]

[a] Department of Geology, Southern Illinois University, Carbondale, IL 62901, USA
[b] Department of Microbiology, Southern Illinois University, Carbondale, IL 62901, USA
[c] Environmental Resources and Policy Program, Southern Illinois University, Carbondale, IL 62901, USA

ARTICLE INFO

Article history:
Received 30 March 2015
Received in revised form
22 July 2015
Accepted 3 August 2015
Available online 6 August 2015

Keywords:
Acid mine drainage
Passive treatment bioreactor
Bioremediation
Bacterial sulfate reduction
Abandoned coal mine

ABSTRACT

Field experiments were conducted over a 460-day period to assess the efficiency of different mixtures of organic substrates to remediate coalmine-generated acid mine drainage (AMD). Five pilot-scale, flow-through bioreactors containing mixtures of herbaceous and woody organic substrates along with one control reactor containing only limestone were constructed at the Tab-Simco site and exposed to AMD ***in situ***. Tab-Simco is an abandoned coal mine near Carbondale, Illinois that produces AMD with pH ~2.5 and notably high average concentrations of SO_4 (5050 mg/L), Fe (950 mg/L), Al (200 mg/L), and Mn (44 mg/L). Results showed that the sequestration of SO_4 and metals was achieved in all reactors; however, the presence and type of organic carbon matrix impacted the overall system dynamics and the AMD remediation efficiency. All organic substrate-based reactors established communities of sulfate reducing microorganisms that contributed to enhanced removal of SO_4, Fe, and trace metals (i.e., Cu, Cd, Zn, Ni) via microbially-mediated reduction followed by precipitation of insoluble sulfides. Additional mechanisms of contaminant removal were active in all reactors and included Al- and Fe-rich phase precipitation and contaminant surface sorption on available organic and inorganic substrates. The organic substrate-based reactors removed more SO_4, Fe, and Al than the limestone-only control reactor, which achieved an average removal of ~19 mol% SO_4, ~49 mol% Fe, 36 mol% Al, and 2 mol% Mn. In the organic substrate-based reactors, increasing herbaceous content correlated with increased removal efficiency of SO_4 (26–35 mol%), Fe (36–62 mol%), Al (78–83 mol%), Mn (2–6 mol%), Ni (64–81 mol%), Zn (88–95 mol%), Cu (72–85 mol%), and Cd (90–92 mol%), while the diversity of the intrinsic microbial community remained relatively unchanged. The extrapolation of these results to the full-scale Tab-Simco treatment system indicated that, over the course of a 460-day period, the predominantly herbaceous bioreactors could remove up to 92,500 kg SO_4, 30,000 kg Fe, 8,950 kg Al, and 167 kg Mn, which represents a 18.3 wt%, 36.8 wt%, 4.1 wt% and 82.3 wt% increase in SO_4, Fe, Al, and Mn, respectively, removal efficiency compared to the predominantly ligneous bioreactors.

The results imply that anaerobic organic substrate bioreactors are promising technologies for remediation of coal-generated AMD and that increasing herbaceous content in the organic substrate matrix can enhance contaminant sequestration. However, in order to improve the remediation capacity, future designs must optimize not only the organic carbon substrate but also include a pretreatment phase in which the bulk of dissolved Fe/Al-species are removed from the influent AMD prior to entering the bioreactor because of 1) seasonal variations in temperature and redox gradients could induce dissolution of the previously formed redox sensitive compounds, and 2) microbially-mediated sulfate reduction activity may be inhibited by the excessive precipitation of Al- and Fe-rich phases.

1. Introduction

Active and historic coal mining operations have left a trail of environmental problems, including coal-generated drainage, which

* Corresponding author. Department of Geology, Southern Illinois University, Carbondale, IL 62901, USA.
E-mail address: lefticar@siu.edu (L. Lefticariu).

http://dx.doi.org/10.1016/j.apgeochem.2015.08.002
0883-2927/

is one of the most pernicious forms of water pollution worldwide (Hedin, 1989; Cravotta, 2008; Palmer et al., 2010). Weathering of coalmine waste often results in the production of acid mine drainages (AMD), which are low-pH, SO_4-, Al-, and heavy metal-rich waters. In the Illinois Basin this has been a significant and costly problem as extensive mining was carried out during the last century (Behum et al., 2011). Concern over the impact to drinking-water resources make remediation of coal-generated AMD imperative in many mining regions around the world (Cravotta, 2008; Baruah and Khare, 2010; Chen et al., 2015). However, remediation of these drainages to the point of meeting the surface water quality standards has proved challenging because of the extreme geochemical characteristics of certain coal-generated AMD (Behum et al., 2011).

Treatment technologies using a combination of biological and geochemical approaches have been used with various degrees of success in many mining districts throughout the world (Neculita et al., 2007; Blowes et al., 2014). Among them, anaerobic organic substrate bioreactors (**AOSB**) rely mainly on biologically-mediated sulfate reduction for pH neutralization (reaction R1), and SO_4 and toxic metal sequestration in insoluble sulfide minerals (reaction R2), with no active addition of chemicals (Johnson and Hallberg, 2005; Neculita et al., 2007; Lindsay et al., 2011; Behum et al., 2011).

$$2CH_2O + SO_4^{2-} \rightarrow 2HCO_3^- + H_2S \quad (R1)$$

$$M^{2+} + H_2S \rightarrow MS + 2H^+ \quad (R2)$$

Additional abiotic and biologically-mediated processes that result in precipitation of hydrated oxide and sulfate phases as well as adsorption on available surfaces also contribute to the overall contaminant attenuation processes (Peretyazhko et al., 2009; Burgos et al., 2012).

Optimal growth conditions for sulfate-reducing bacteria (**SRB**) comprise anaerobic, alkaline settings with moderate salt and metal content. Factors limiting SRB activity in AOSB treatment systems include low-pH conditions as well as the availability of suitable electron donors, which may be either simple organic compounds or molecular hydrogen (H_2). Recent studies have shown that microbial sulfate reduction (**MSR**) activity is possible in low-pH settings such as acidic lakes and soils, wetlands, mine tailings, and bioreactors (Praharaj and Fortin, 2004; Neculita et al., 2007; Koschorreck, 2008; Senko et al., 2009; Moreau et al., 2010; Meier et al., 2012; Sánchez-Andrea et al., 2014). In terms of electron donors, SRB utilize H_2 or simple organic compounds as a carbon and energy source and rely on other anaerobic bacteria (i.e., fermenters) to break down complex organic compounds to products such as H_2, lactate and pyruvate (Gibert et al., 2004; Rabus et al., 2013).

The selection of appropriate electron donors is essential when designing AOSB technology to sustain long-term, viable SRB communities (Cocos et al., 2002). Previous research has tested a wide range of organic matter (OM) substrates for AOSB, including spent mushroom compost (Newcombe and Brennan, 2009; Neculita et al., 2011), plant materials (Chang et al., 2000; Harris and Ragusa, 2001; Lindsay et al., 2011), chitin (Robinson-Lora and Brennan, 2010), straw (Koschorreck et al., 2002), methanol (Glombitza, 2001), and ethanol (Greben et al., 2000). Several laboratory studies have reported that combining cellulosic (wood chips, sawdust, etc.) and mixed organic substrates (manure, compost, brewing wastes) resulted in improved AMD treatment in long-term experiments (Zagury et al., 2006; Lindsay et al., 2011). To further demonstrate the benefit of mixed-substrate bioreactors, Neculita et al. (2011) reported that after 70 days mixed organic waste substrates harbored $<10^4$ more SRB than cellulosic wastes, despite the release of up to 44% more total organic carbon from cellulosic substrates. In the case of AOSB, even though simple organic substrates may be more effective at stimulating SRB in the short-term, complex organic substrates could provide a long-term reservoir of simple organic compounds for SRB utilization due to their sequential breakdown (Zagury et al., 2006).

Despite increasing evidence that a mixed-substrate organic source can provide a long-term carbon and energy source for SRB in AOSB, no data are available to assess the relative effectiveness of variable organic layer constituents ***in situ***. The current study evaluated the use of various proportions of herbaceous (i.e. grass clippings, spent brewing grain, leaf compost) and ligneous (i.e. maple wood chips and sawdust) mixtures for optimal, long-term remediation of AMD by AOSB technology. The results indicated that the addition of OM to a limestone substrate greatly increased the coalmine-generated AMD remediation efficiency by simulating MSR, which also was the highest for the predominantly herbaceous AOSB reactors.

2. Experimental approach

2.1. Experimental setup

Field experiments were conducted over a 460-day period at the Tab-Simco (TS) site to evaluate the effect of simple versus complex carbon sources on remediation efficiency of coal-generated AMD using *in situ* continuous-flow reactors. Details of field site, experimental design, and field and laboratory methods were described in Walters (2013). Briefly, five flow-through bioreactors containing various mixtures of herbaceous and woody organic substrates (R2–R6) along with one control reactor containing only limestone (R1) were constructed using six 0.21 m^3 polyethylene barrels at the TS site. The site is an abandoned coal mine located 6 km SE of Carbondale, Illinois, USA, and consists of ~121,406 m^2 of underground mine works that have been discharging AMD through several man-made seeps (Behum et al., 2011; Burns et al., 2012). The influent AMD was channeled from the TS main seep into a small impoundment constructed using a weir system. This approach increased the hydraulic head allowing a continuous flow of AMD from the TS main seep through a pipe system into each reactor for the duration of the experiment (Walters, 2013). The top of each reactor was cut open to allow the influent AMD to pond, thus simulating an acid impoundment analogous to the full-scale TS remediation system. Three sampling ports with PVC screw caps and butyl stoppers were inserted at 0.2 m intervals to allow for sampling porewater with a syringe at various depths within the reactor. The effluent exit ports were installed at the bottom of each reactor and fitted with valves to allow for the maintenance of a continuous effluent flow out of each reactor at a rate of ~5 mL/min, proportional to the flow rate of the full-scale TS remediation system (Behum et al., 2011).

The OM-based reactors (R2–R6) were built by laying 25 L (~48 Kg) of limestone at the bottom of the barrels and then adding mixtures of herbaceous (hemicellulose) and woody (ligneous) organic substrates with a total uncompressed volume of 125 L. The role of the limestone layer was to produce alkalinity and maintain permeability. Additionally, 12 L of livestock manure and 7 L of whey powder were mixed into the organic substrate as a microbial inoculum to provide an immediate source of low molecular weight organic compounds (Table 1). A volume of 54 L was left empty and open to the atmosphere at the top of the bioreactors to provide space for the AMD to pond. Reactor R1, simulating an open limestone treatment system, was designed as a control and it contained only 25 L of limestone as its total solid volume (Table 1). The experimental bioreactors were monitored for 460 days from August 2012 to November 2013. Table 1 lists the substrate composition of

Table 1
Composition of the reactive mixtures used for pilot-scale R1–R6 reactors.

Substrate[b]	Reactor 1 (0:0)[a]	Reactor 2 (10:90)[a]	Reactor 3 (30:70)[a]	Reactor 4 (50:50)[a]	Reactor 5 (70:30)[a]	Reactor 6 (90:10)[a]
LC[c]	0	4%	12%	20%	28%	36%
SBG[c]	0	2%	6%	10%	14%	18%
GC[c]	0	4%	12%	20%	28%	36%
Total Herbaceous	**0**	**10%**	**30%**	**50%**	**70%**	**90%**
MWC[c]	0	45%	35%	25%	15%	5%
MSD[c]	0	45%	35%	25%	15%	5%
Total Ligneous	**0**	**90%**	**70%**	**50%**	**30%**	**10%**
SWP[d]	0	2	2	2	2	2
LM[d]	0	4	4	4	4	4
LS[d]	25	25	25	25	25	25

[a] (X:Y) represents ratios of complex to simple substrates as defined in the text.
[b] Substrate: Leaf Compost (LC), Spent Brewing Grain (SBG), Grass Clippings (GC), Maple Wood Chips (MWC), Maple Sawdust (MSD), Sweet Whey Powder (SWP), Livestock Manure (LM), Limestone (LS).
[c] Expressed as volume % of the total compost volume.
[d] Number indicates liters of material added.

each bioreactor fill.

2.2. Water sampling and analysis

Water samples were collected from the AMD influent, acid pond, and effluent in 250 ml polyethylene bottles biweekly during the summer months and monthly during the winter months. The standards and reagents used in the field and laboratory were prepared using deionized (D)I water from Milli-Q/Milli-Q Ultra Plus (>18 MΩ cm^{-1}) with a UV photo-oxidation water system. Field parameters, including pH, temperature, specific conductance (SC), oxidation reduction potential (ORP), and dissolved oxygen (DO) were measured on unfiltered samples immediately following sample collection using a Hanna® multi-sensor probe. The pH electrode Hanna HI769828-1 field probe (pH/ORP) was calibrated with Orion pH 1.68, 4.01, and 7.00 buffers and then checked against pH 10 buffer. ORP was measured using a factory calibrated Hanna HI769828-1 Ag/AgCl probe. DO was determined with a Hanna HI769828-2 amperometric probe calibrated to onsite atmospheric oxygen as 100% DO. AMD influent and effluent rates were quantified using a 10 ml volumetric flask and timed on a stop watch. Samples selected for laboratory analyses were filtered through 0.45 μm cellulose acetate filter papers (Millpore® HAW) and stored at 4 °C if not analyzed immediately after collection. Alkalinity was measured to the end-point (pH = 4.5) using a Hach™ digital titrator (Model AL-DT), standardized sulfuric acid, and a Hanna® multi-sensor probe. Dissolved sulfide and ferrous iron measurements were carried out within 5 h of sampling on unacidified samples using a UV-VIS spectrophotometer (Hach® DR 3900) via USEPA methylene blue and 1–10 phenanthroline methods, respectively. The samples were subsequently analyzed for dissolved anions (i.e., SO_4^{2-}) by means of ion chromatography (Dionex® ICS 2000) using an IonPac® AS18 anion-exchange column. Samples for cation analyses (i.e., Al, Ca, Cd, Cu, Fe, Mn, Ni, and Zn) were preserved with trace-metal grade HNO_3 and analyzed by atomic absorption spectrophotometry (Hitachi Z-2000 Tandem AA). Teledyne plasmapure® stock aqueous metal standards were used for calibration. Dissolved Al concentrations were measured on a Hach® DR 3900 spectrophotometer using the acidified sample (5 wt/v% nitric) which was also prepared for AAS analyses. Additionally, duplicate samples, acid blanks, and DI water samples were analyzed at the AcmeLabs Analytical Laboratories S.A. in Vancouver, Canada, for quality control. Anion and metal concentrations were below analytical detection limits in acid blacks and DI water. The standard deviation for duplicate sample analyses was consistently <5% for both anions and cations. Standard deviation bars are not displayed on figures as the symbol size for individual data points is larger than the standard deviation of the measurement.

Geochemical modeling of influent and effluent data was performed using the *SpecE8* module of the program *Geochemist's Workbench®* developed at the University of Illinois at Urbana–Champaign. When modeling acidic coal mine drainage it is often difficult to obtain a desirable anion–cation balance. Although in most cases the balance was <5%, whenever it was exceeded and water quality dataset was otherwise determined to be accurate and all significant parameters were included, we allowed *SpecE8* to adjust the balance by changes in SO_4 levels. An exception to this was in the early modeling period when *SpecE8* adjusted the balance when necessary by small changes in Cl levels. Geochemical modeling was also used to calculate other important parameters such as the saturation index (SI) (Walters, 2013).

2.3. Stable isotope measurements

Dissolved sulfate was recovered from filtered, acidified, water samples (50 mL) by addition of 0.2 M $BaCl_2$ solution and precipitation of $BaSO_4$. Recovered $BaSO_4$ was dried, weighed, and retained for isotope analysis (Lefticariu et al., 2006). For sulfur stable isotope measurements, aliquots of $BaSO_4$ were loaded into tin cups, mixed with V_2O_5, and combusted on-line in an EA 1110 elemental analyzer at 1400 °C. SO_2 pulses in He carrier gas passed through a 1010 °C oxidation–reduction column, an $MgClO_4$ water trap, and a 0.8 m Costech packed column before entering a Finnigan MAT 252 mass spectrometer. The analytical precision (±1σ) of $\delta^{34}S$ values was < ± 0.05‰, whereas sample reproducibility was typically ± 0.15‰. All isotopic data are expressed in customary $\delta^{34}S$ in parts per thousand (‰) relative to Vienna Cañon Diablo Troilite (V-CDT). The following international standards were used for calibration: IAEA–S1 = −0.3‰, IAEA–S2 = +21.6‰, IAEA–S3 = −31.3‰, NBS-127 = +20.3‰.

2.4. Porewater microbial community analysis

Porewater samples were extracted in duplicate from each reactor substrate at each sampling port with a 50 ml syringe, placed on ice, stored at 4 °C, and processed within 48 h of returning to the lab (Pugh, 2013). Following centrifugation at 5000 × g for 15 min to pellet solid particles, the liquid containing biomass samples were collected on 0.2 μm sterile analytical test filters by vacuum filtration. DNA from the filters was extracted using the FastDNA® SPIN Kit for Soil (MP Biomedicals). The resulting DNAs were subjected to 16S rRNA Tag-Encoded FLX Amplicon Pyrosequencing (bTEFAP) by Molecular Research LP (Shallowater, Texas) using 16S universal Eubacterial primers 27F (5′-AGA GTT TGA TCM TGG CTC AG- 3′) and

530R (5′-CCG CNG CNG CTG GCA CS- 3′) and the Genome Sequencer FLX System (Roche). Raw sequences were depleted of barcodes, primers, and sequences <200 bp prior to processing using a proprietary analysis pipeline (www.mrdnalab.com) and the Quantitative Insights into Microbial Ecology (QIIME) open source software package (Caporaso et al., 2010). Relative class abundance was plotted based on operational taxonomic units (OTUs) chosen at a 97% sequence similarity cutoff. The current study focuses on those porewater samples collected at the lowest sampling port of reactors R1–R6 (Pugh, 2013).

3. Results

Geochemical data of the AMD influent and the R1–R6 effluents collected during the 460-day field experiments are plotted in Figs. 1–3 and tabulated in Appendix 1 (Tables S1–S7).

3.1. Drainage characteristics – physicochemical parameters

For the duration of this study, each of the reactors R1–R6 received AMD at an average rate of ~5 mL/min. Ambient air temperature at the TS site varied between −13 and +35 °C and effluent temperature in R1–R6 ranged from +5 to +28 °C. Daily precipitation, up to 6.73 cm, caused short-term fluctuations in the AMD physicochemical parameters, however, these changes were short-lived and of minor significance when compared to the long-term trends.

The pH of the AMD influent remained relatively constant for the duration of this study, with an average pH value of 2.7 (Fig. 1a; Table S1). The average pH value of the R1 effluent was 3.3, a value slightly above that of the influent AMD. Within the bioreactors R2–R6, the effluent pH values were constantly higher than those of R1, increasing from initial values of ~4.5 up to ~6.4 during the fall of 2012, then gradually decreasing during the spring of 2013 and fluctuating around ~4.6 during the summer and ~4.0 during the fall of 2013.

Total alkalinity was measured only in effluent samples that displayed pH values >4.5, therefore the AMD influent and R1 effluents were documented as displaying no titratable alkalinity (Fig. 1b). A large increase in alkalinity was recorded in R3, R4, and R5 with reactors R3 and R4 reaching alkalinity as high as 4200 mg/L as $CaCO_3$ during the second week of the experiments. Continued measurements identified that high levels of alkalinity were not maintained and the effluent alkalinity in the R2–R6 decreased to values below 500 mg/L as $CaCO_3$ by November 2012, concentration values that were maintained for the duration of the experiment.

Similar ORP values were recorded for the AMD influent and R1 effluent (Fig. 1c), with lower ORP values ($ORP_{average}$ = 100 mV) during the initial six months (August, 2012- early February, 2013) and higher ORP values ($ORP_{average}$ = 300 mV) during the following months (late February–November, 2013). Divergent trends on ORP were recorded for R2–R6, with effluent ORP values up to 400 mV lower in R2–R6 than those measured in R1 effluent during the last 10 months of the experiment.

Large variations of the DO values were recorded in the AMD influent and R1–R6 effluent samples (Fig. 1d). In R2–R6, the initial decrease in DO values was followed by an increase during the cold temperature months (T < 10 °C). During the warm months of 2013, variable levels of DO were measured in the AMD influent and R1–R6 effluent samples (Fig. 1d).

3.2. Drainage characteristics – major and trace element chemistry

The influent AMD was highly acidic with high average concentrations of SO_4 (5050 mg/L) and metals, including Fe (932 mg/L), Al (200 mg/L), Mn (44 mg/L) and Ca (307 mg/L) (Table S1). Substantial

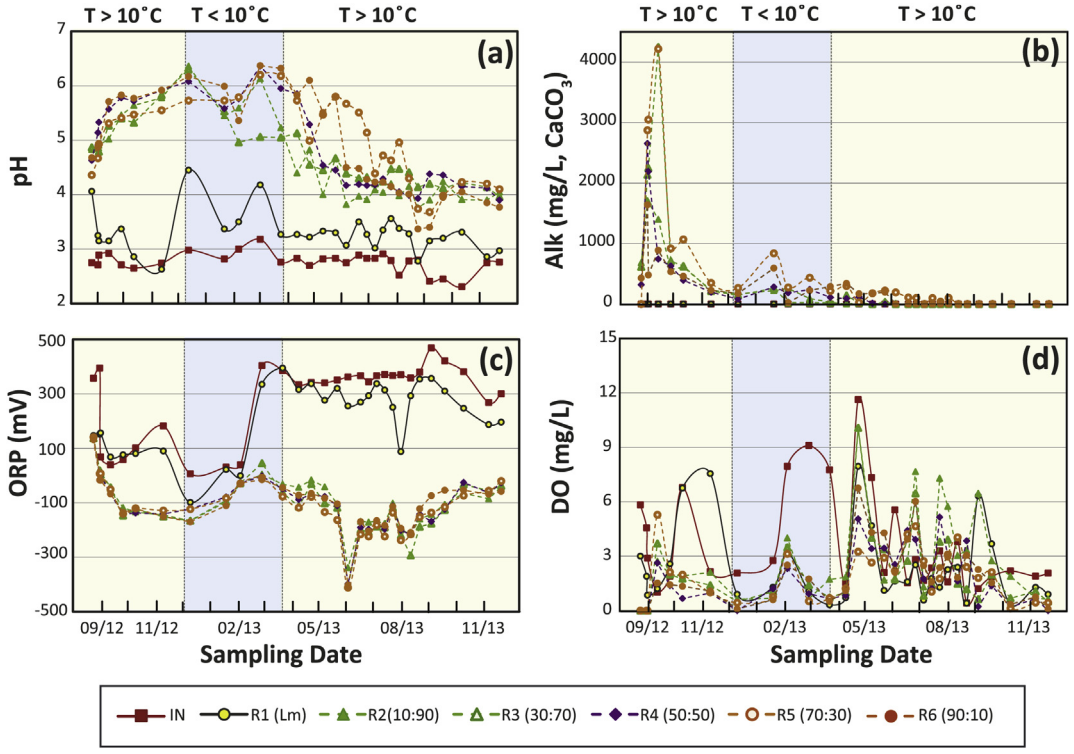

Fig. 1. Temporal trends for (a) pH (b) alkalinity (Alk), (c) oxidation reduction potential (ORP), and (d) dissolved oxygen (DO) measured in the influent AMD (IN), the control limestone reactor (R1), and organic substrate-based reactors (R2-R6) during the 460-day field experiments. For R2-R6, (X:Y) represents ratios of complex to simple organic substrates as defined in the text.

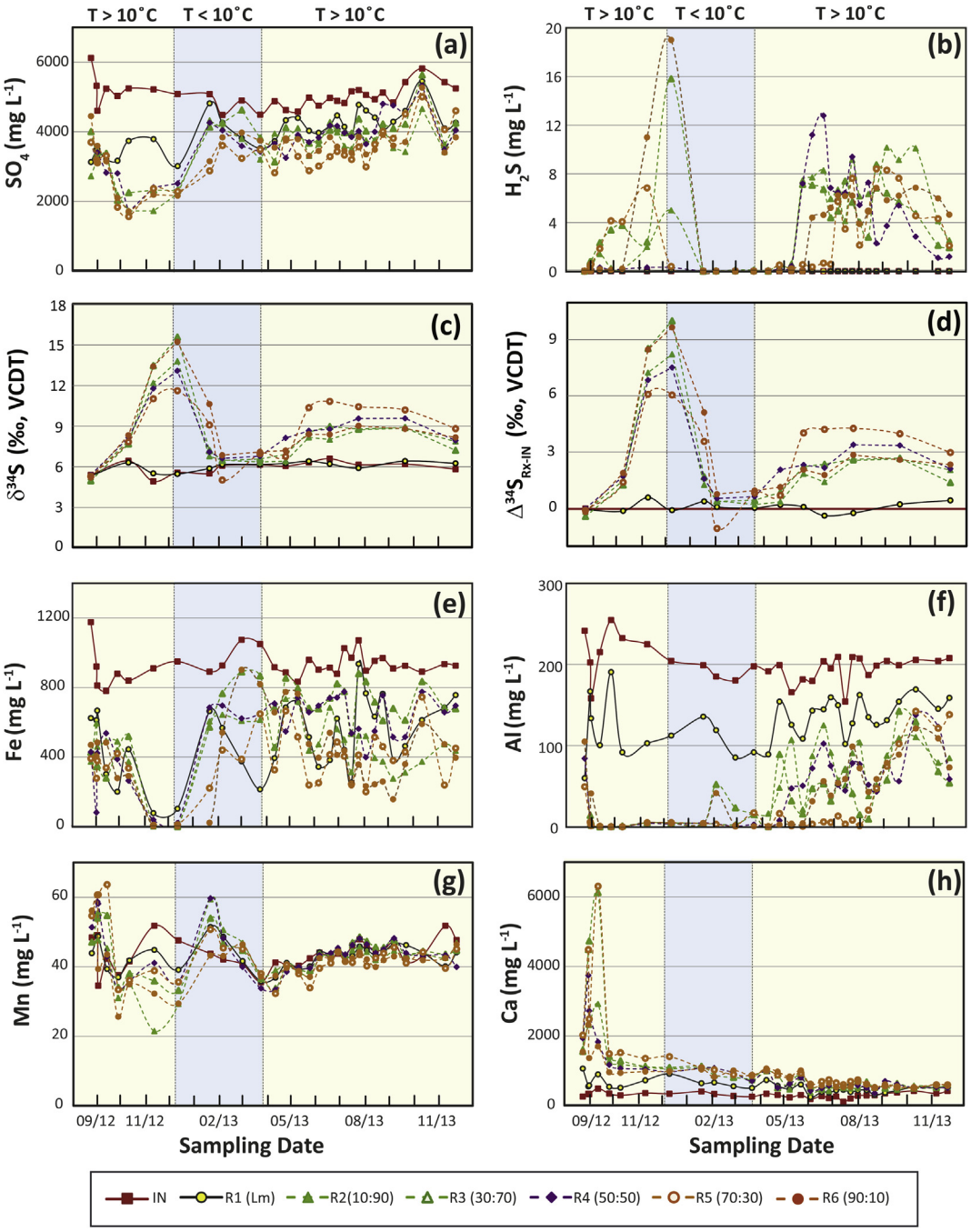

Fig. 2. Temporal trends for the concentrations of dissolved (a) dissolved sulfate (SO_4^{2-}), (b) sulfide (H_2S) (c) stable sulfur isotope values of dissolved sulfate ($\delta^{34}S$), (d) stable sulfur isotopic differences between each reactor effluent SO_4 and and influent SO_4 ($\Delta^{34}S_{Rx-IN}$), (e) iron (Fe), (f) aluminum (Al), (g) manganese (Mn) and (h) calcium (Ca), in the influent AMD (IN), the control limestone reactor (R1), and organic substrate-based reactors (R2–R6) during the 460-day field experiments. For R2–R6, (X:Y) represents ratios of complex to simple organic substrates as defined in the text. The error bars for $\delta^{34}S$ values are smaller than the size of data symbols.

heavy metal enrichments were also present with elevated average concentrations for Ni (2 mg/L), Zn (3.4 mg/L), Cu (80 μg/L), and Cd (20 μg/L). SO_4 concentrations in R1–R6 were considerably lower compared to those in the AMD influent and they followed similar temporal patterns with lower levels recorded during the fall of 2012 followed by a subsequent steady increase (Fig. 2a). H_2S was detected only in reactors R2–R6 during warm months (T > 10 °C) (Fig. 2b). During our experiments, sulfur isotope values of the influent SO_4 ($\delta^{34}S_{IN}$) displayed minimal variations of <0.9‰ (Fig. 2c). Sulfur isotopic differences between each reactor effluent SO_4 and influent SO_4 are reported as isotopic differences in capital delta notation $\Delta^{34}S_{Rx-IN}$ (Fig. 2d). In case of reactor R1, the $\Delta^{34}S_{IN-R1}$ values ranged from −0.38 to +0.59‰, which were relatively small. In contrast, the bioreactors R2–R6 displayed $\Delta^{34}S_{Rx-IN}$ values which were highly variable, with values up to +10‰ during the fall of 2012, small (±0.5‰), or even negative (−1.06‰) during the winter of 2012–2013, and up to +4.5‰ during the summer and fall of 2013 (Fig. 2d).

Metal sequestration patterns in R1–R6 effluents were dependent on the presence of OM, with significantly higher sequestration of Al, Ni, Zn, Cu, and Cd in reactors R2–R6 as compared to those recorded in reactor R1 effluents (Fig. 2 e–h; Fig. 3). A suite of metals

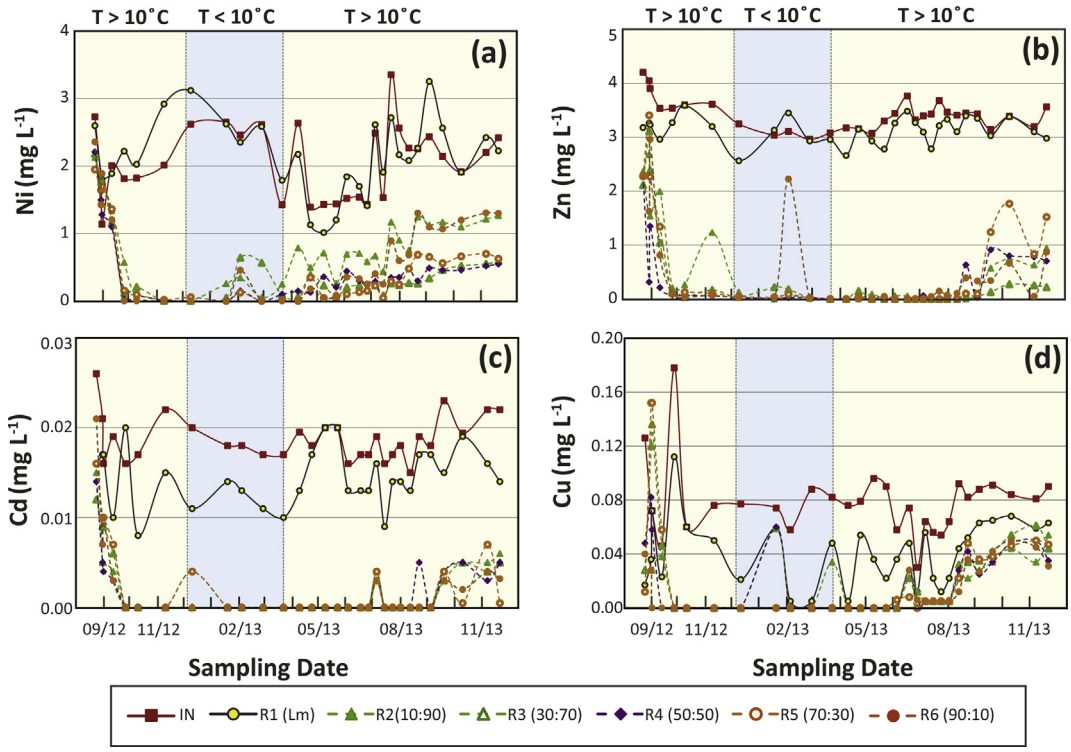

Fig. 3. Temporal trends the concentrations of dissolved (a) nickel Ni (b) zinc (Zn), (c) cadmium (Cd), and (d) copper (Cu) in the influent AMD (IN), the control limestone reactor (R1), and organic substrate-based reactors (R2–R6) during the 460-day field experiments. For R2–R6, (X:Y) represents ratios of complex to simple organic substrates as defined in the text.

were removed to below detection limits (i.e., Al, Ni, Zn, Cu, and Cd) in R2–R6, especially during the first months of treatment. Iron concentrations followed similar temporal trends in all reactors, with significantly lower values measured in effluents during the fall of 2012 and increased, variable values afterwards (Fig. 2e). Manganese concentrations decreased in treated R1–R6 effluents compared to influent AMD during the initial four months of the experiments and, after a small reversal of this trend during cold months, remained in close correspondence to AMD values afterwards (Fig. 2g). Calcium concentration trends in R2–R6 effluents were similar to those of alkalinity, with significantly higher values immediately after exposure to AMD influent, up to 6300 mg/L in R2–R6 and 1060 mg/L in R1. Calcium concentrations measured in the R2–R6 effluents were consistently greater relative to those measured in R1 effluent. Such pronounced increases in Ca concentration were short-lived as they decreased to >1500 mg/L Ca in all bioreactors after just one month (Fig. 2h) and continuously declined thereafter.

3.3. Microbial community analysis of substrate porewater

DNA sequencing data from the August 2012, May 3013, and October 2013 time points indicated that the microbial community present in the substrate porewater collected at the lowest sampling port of reactors R2–R6 (organic substrate) was different than that of the porewater of the limestone control reactor (R1) (Fig. 4). After initial reactor construction in August of 2012, the microbial communities of reactors R2–R6 contained representatives of the *Bacilli*, *Clostridia*, and *Bacteriodia* classes. These classes are commonly found in livestock manure, which was used as the microbial inoculum for reactors R2–R6. As the field trial progressed, the microbial community in the organic substrate-containing bioreactors gradually shifted in that the sequences related to members of the *Gammaproteobacteria*, *Betaproteobacteria*, and *Alphaproteobacteria* classes increased in abundance. However, sequences related to the *Bacteriodia* and *Clostridia* classes were still more abundant in the organic substrate-containing bioreactors than in the limestone-only control for the May time point. While the molecular data indicated that the organic substrate composition did not have an effect on the community dynamics of the experimental bioreactors, the presence of *Deltaproteobacteria* and *Clostridia* classes, which possess SRB members capable of generating H_2S, was detected in R2–R6 for the May 2013 and October 2013 time points (Fig. 4).

4. Discussion

During the 460-day field experiments, important reductions in the concentrations of SO_4, Fe, Al, and heavy metals were recorded in the effluents of control limestone reactor R1 and bioreactors (R2–R6) as compared to those in the AMD influent. The overall extent of contaminant removal was primarily a function of: (1) presence of organic substrate matrix, (2) proportion of herbaceous substrate in the organic substrate mixture, (3) environmental conditions within the reactors, and (4) seasonal variations of physicochemical parameters.

4.1. Mechanisms for sulfate removal

SO_4 removal in R1–R6 was pH dependent (Fig. 5a) and achieved through a combination of biotic and abiotic processes that included microbially-mediated reduction followed by precipitation of insoluble sulfides, precipitation of SO_4-rich phases, and absorption of SO_4 on mineral and organic substrate surfaces.

In reactor R1, which lacked an organic substrate matrix, acidic conditions were established immediately after exposure to AMD. Overall, the presence of limestone in R1 contributed to a modest

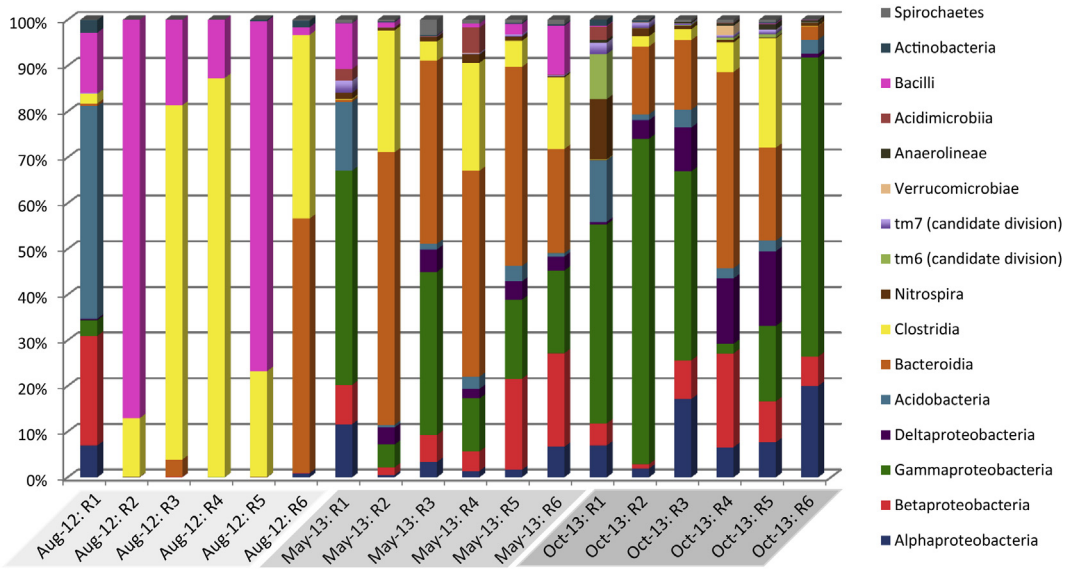

Fig. 4. Relative bacterial class abundance in each reactor as determined from 16S rRNA gene pyrosequencing of DNA from August 2012, May 2013, and October 2013. The abundance levels are based on OTUs chosen at a 97% sequence similarity cutoff and filtered by taxa detected >0.1% of the total.

increase in effluent pH, with pH values reaching only ~1 unit over those of the AMD influent (Fig. 1a), and no alkalinity production (Fig. 1b). These trends were probably caused by the passivation of limestone due to the formation of SO_4-rich precipitates, which restricted limestone dissolution (Fig. 2h) and alkalinity production (Fig. 1b). This interpretation is consistent with previous studies which showed that passivation of limestone by SO_4-rich precipitates can occur hours after exposure to AMD (Hedin et al., 1994; Cravotta and Trahan, 1999; Hammarstrom et al., 2005; Huminicki and Rimstidt, 2008). Conversely, limited limestone passivation occurred in bioreactors (R2–R6), which resulted in effluents with significantly higher pH (Fig. 1a), alkalinity (Fig. 1b), and Ca concentrations (Fig. 2h) over those of limestone reactor R1. Direct correlation between the Ca concentration and pH in the R2–R6 effluents (Fig. 5b) suggest that lower passivation of limestone resulted in higher limestone dissolution rates and thus higher alkalinity production. Since all reactors had the same volume of limestone, the presence of OM matrix was critical in reducing

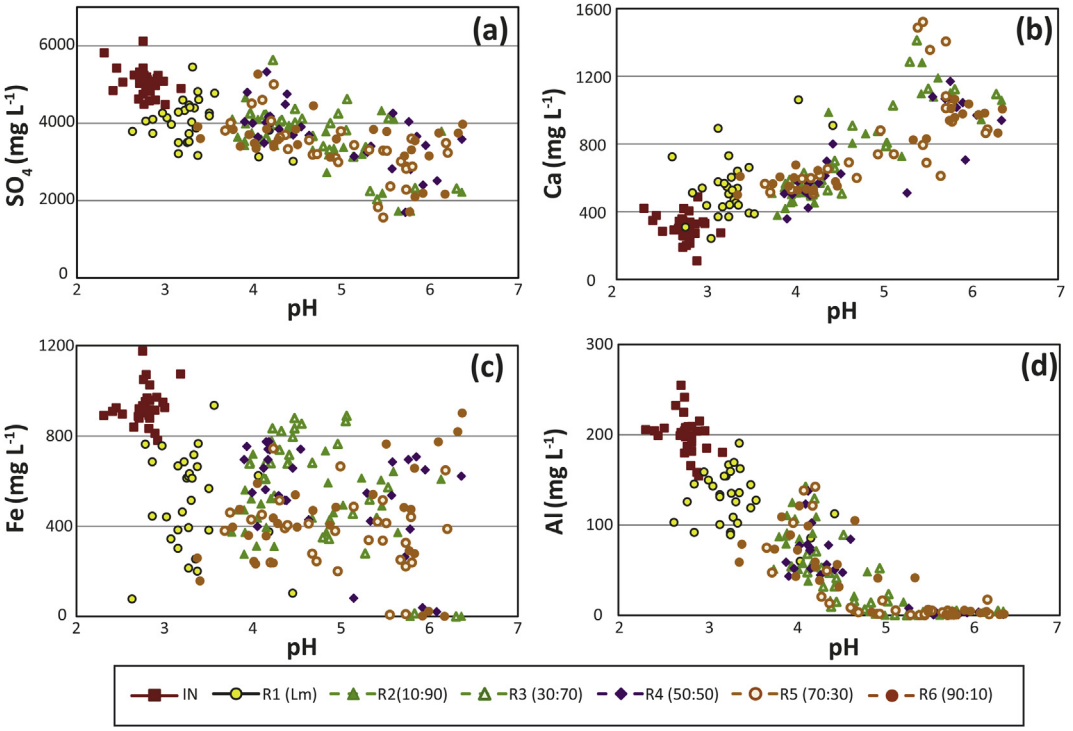

Fig. 5. Comparison of pH values and the concentrations of dissolved (a) sulfate SO_4^{2-}, (b) calcium Ca, (c) iron Fe, and (d) aluminum Al in the influent AMD (IN), the control limestone reactor (R1), and organic substrate-based reactors (R2–R6) during the 460-day field experiments. For R2–R6, (X:Y) represents ratios of complex to simple organic substrates as defined in the text.

limestone passivation, due to AMD mitigation within the OM matrix before passing through the limestone layer (Zagury et al., 2006; Johnson and Hallberg, 2005).

In reactor R1, microbiological (Fig. 4) and geochemical data, including pH (Fig. 1a), alkalinity (Fig. 1b), ORP (Fig. 1c), H_2S levels (Fig. 2b), and $\Delta^{34}S_{IN-R1}$ values (Fig. 2d) indicate that no MSR activity occurred for the duration of this study. In bioreactors R2–R6, conditions favorable for MSR activity, including neutral pH (Fig. 1a), high alkalinity (Fig. 1b), and decreased ORP (Fig. 1c) and DO (Fig. 1d) values, were rapidly established. During the first 6–10 days after the inoculation, the decreasing SO_4 (Fig. 2a) and increasing H_2S (Fig. 2b) concentrations, indicate the presence of effective MSR processes. Bacterial sulfate reduction can produce large sulfur isotope effects by preferentially incorporating ^{32}S into the H_2S and leaving a ^{34}S-enriched SO_4 reservoir into the solution. However, the magnitude of sulfur isotope fractionation during sulfate reduction depends on the concentration of dissolved sulfate. Systems with dissolved sulfate concentration <1 mM, such as those of R2–R6, generally produce small sulfur isotope fractionations (<3‰) (Canfield, 2001). The positive, large $\Delta^{34}S_{Rx-IN}$ values calculated for the warm months (T > 10 °C) in bioreactors R2–R6 suggests increased MSR activity.

The cellulolytic and fermentative organisms (e.g. *Bacilli*, *Clostridia*, *and Bacteriodia*) related to livestock manure used to inoculate the reactors (Pugh, 2013), presumably provided a source of simple OC for SRB (Pruden et al., 2007; Wirth et al., 2012; Sun et al., 2015). In time, the lignin/cellulose ratio of the substrate may have increased as a consequence of bacterial activity because lignin degrades slower than cellulose especially in anaerobic conditions (Pérez et al., 2002; Komilis and Ham, 2003; Li et al., 2009).

While the community structure in the reactors appeared to be more dependent on temporal and seasonal factors than the organic substrate composition, the DNA sequencing data suggested that members of *Clostridia* and *Deltaproteobacteria* classes, known to contain SRB (Campbell and Postgate, 1965; Druschel et al., 2004; Meyer and Kuever, 2007; Pruden et al., 2007; Sallam and Steinbüchel, 2009) were stimulated in reactors R2–R6, with the largest corresponding population detected in October 2013 (Fig. 4). Besides the presence of sequences related to *Clostridia* and *Deltaproteobacteria*, the bacterial communities detected in reactors R2–R6 at the end of the experiment were more similar to that of the limestone R1 control (Fig. 4). The stimulation of members of the *Gammaproteobacteria*, *Betaproteobacteria*, and *Alphaproteobacteria*, which possess members capable of iron cycling and sulfur oxidation (Baker and Banfield, 2003; Hedrich et al., 2011; Johnson et al., 2012), suggests that precipitate formation within the organic substrate-containing reactors may have occurred over the duration of the field trial possibly limiting OC substrate availability. While anaerobic conditions are necessary for active sulfate reduction and microaerophilic conditions are necessary for iron and sulfur oxidation under low-pH conditions, the concurrence of these two disparate metabolisms may be explained by microniche or biofilm formation within the system (Bertis and Ziebis, 2010; Desai et al., 2013; Ziegler et al., 2013). Future studies will require OC analysis of the reactors as well as further research into the attached versus planktonic microbial community to determine the dynamics occurring within the bioreactors.

4.2. Mechanisms for metal removal

In the influent AMD, both Fe(II) and Fe(III) were highly soluble under the low-pH (pH < 3) conditions (Fig. 5c). In reactors R1–R6 (pH > 3), Fe removal was likely achieved via microbially-mediated sulfate reduction followed by sulfide mineral precipitation (R2–R6), solid-phase co-precipitation (R1–R6), and surface absorption (R1–R6). Sorption of Fe(III) on lignin would be favored within the pH and temperature ranges of the experiment (Merdy et al., 2002). The concentrations of Fe and SO_4 in R2–R6 effluents were directly correlated ($r^2 = 0.45$, $p = 0.021$) suggesting that the cycles of these two elements were intrinsically connected.

Intriguingly, regardless of the presence and type of OM, Fe concentration in R1–R6 effluents displayed similar temporal trends (Fig. 2e), with no overall correlation with pH values (Fig. 5c). In SO_4–Fe dominated media, Fe redox cycling and consequently Fe sequestration, depends on a tight interplay between abiotic and biotic processes, the latter mediated by various microorganisms that can catalyze the dissimilatory oxidation of Fe(II) (FeOB), or reduction of Fe(III) (FeRB), or can do both depending on the prevailing environmental conditions. In the acid impoundment of the reactors R1–R6, common AMD community members like the acidophilic FeOB of the genera *Acidimicrobiaceae*, *Alicyclobacillaceae* and *Acerobacteraceae* (Neculita et al., 2007; Pugh, 2013) likely oxidized Fe(II) to Fe(III). This activity has been shown to subsequently hydrolyze and precipitate a series of crystalline and poorly crystalline phases (Senko et al., 2008; Walters, 2013), which would have sequestered Fe within the reactors. Fe(III) hydrolysis and precipitation reactions generate protons and thus produce acidity (Majzlan and Myneni, 2004; Lefticariu et al., 2006; Nordstrom, 2011). Geochemical modeling of R1–R6 effluents predicted precipitation (SI > 0) of nano-crystalline $Fe(OH)_3$, goethite (α-FeOOOH), K-jarosite ($KFe^{3+}{}_3(OH)_6(SO_4)_2$), schwertmannite $Fe_8O_8(OH)_6SO_4$, gypsum ($CaSO_4{}^*2H_2O$) and Cu/Zn-Ferrite ($Zn_{1-x}Cu_xFe_2O_4$). Poorly-crystalline precipitates (i.e., schwertmannite) tend to transform into more thermodynamically stable (hydr)oxides such as goethite (Bigham and Nordstrom, 2000; Gagliano et al., 2004; Cornell and Schwertmann, 2003; Jolivet et al., 2004), with subsequent release of structural and adsorbed species back into solution (Rose and Ghazi, 1997; Caraballo et al., 2013). These dynamic transformations can be both abiotic and biologically-mediated and occur predominantly in systems with fluctuating redox conditions (Hansel et al., 2003; Borch et al., 2009), such as those of R2–R6 (Fig. 1c). FeOB can oxidize a variety of reduced inorganic Fe compounds (Zachara et al., 2002; Lentini et al., 2012; Nancucheo and Johnson, 2012) using OM as electron donor (Adams et al., 2006; Becerra et al., 2009; Coggon et al., 2012). Within the reactors R2–R6, pyrite and monosulfides were predicted to form under anaerobic conditions (Walters, 2013), thus iron sulfide likely contributes to Fe removal. In R2–R6, an increase in sequences related to *Alphaproteobacteria* and *Deltaproteobacteria* (Pugh, 2013), which possess dissimilatory Fe-reducing members, indicate that these organisms contributed not only to a build-up of Fe(II) but also to inorganic production of bicarbonate alkalinity.

Aluminum sequestration occurred mainly as Al amorphous phases and adsorption (reversible) to SO_4-rich precipitates and OM. Geochemical modeling of R1–R6 effluents predicted the precipitation (SI > 0) of a mixture of amorphous Al hydroxide ($Al(OH)_3$) and basaluminite ($Al_4(SO_4)(OH)10{\cdot}5H_2O$). The pH had a strong influence on Al removal from solution (Fig. 5d), with higher Al mobility associated with lower pH (Bigham and Nordstrom, 2000). In R1, minor increases in pH resulted in a significant decline in Al concentrations, as a pH increase to 4.0 corresponded to over 50 mol % Al removal from influent AMD. In R2–R6, increasing the pH above 5.0 resulted in 100 mol% Al removal in the majority of samples. Decreasing effluent pH in R2–R6 during the last six months of the field experiments reversed this trend (Fig. 2f).

Divalent Mn ion, the main Mn species in the influent AMD, is relatively stable over a wide range of redox and pH values (Santelli et al., 2010). Oxidative hydrolysis of soluble Mn(II) and precipitation

of stable Mn(III/IV) oxides, catalyzed by abiotic and biotic processes (Cravotta and Trahan, 1999; Hallberg and Johnson, 2005; Santelli et al., 2010), is favored at pH > 8 (Luan et al., 2012). None of these conditions prevailed in our experiments (i.e., pH < 6.5) thus the minimal Mn attenuation observed during the sampling period, except at the very beginning when the dissolved Ca concentrations in the effluents were the highest and also during the coldest period, likely occurred via adsorption on OM rather than on metal precipitates (Fig. 2g and h). Limited and Ca concentration-dependent Mn adsorption on lignin can take place at ambient temperature and pH values similar to that of the bioreactor experiments (Merdy et al., 2002). Likewise, the sorption of Mn on metal precipitates, such as $Al(OH)_3$, for example, is much reduced at pH below 7.5 (Wang et al., 2012).

The mobility of trace metals (Ni, Zn, Cd, and Cu) in aqueous systems dominated by Fe and SO_4 (R1–R6), can be controlled by multiple mechanisms (Walters, 2013) including physical or chemical adsorption on OM (Reddad et al., 2002; Davranche et al., 2013), solid-phase precipitates (DiToro et al., 1992; Burgos et al., 2012), co-precipitation (Lee et al., 2002; Gagliano et al., 2004), or substituting for Fe or SO_4 in the Fe oxyhydroxide structure (Gerth, 1990; España et al., 2006). Divalent metals display sorption isotherm edges that vary with pH and typically sorb on Fe oxyhydroxide from most strongly to less strongly as Cu > Cd > Zn > Ni (Stumm and Morgan, 1996). The pattern and extent of sorption depend on the nature and concentration of the substrate sorbent (Brown and Parks, 2001), thus it is expected to have a different patterns for various inorganic phases and organic substrates present in R2–R6. It is expected the adsorbtion of heavy metals on the lignocellulosic substrate present in the bioreactors to be an important, long-term heavy metal removal mechanism at the pH of these experiments (Perez et al., 2006; Guo et al., 2008; Quintana et al., 2008; Thirumavalavam et al., 2009), perhaps with lignin adsorbing more than cellulose. Moreover, under low-pH conditions, as was often the case of R1–R6, surface-bound SO_4 can also increase heavy metal sorption through the formation of surface complexes (Swedlund et al., 2009). Conversely, mineral transformation can induce trace metal mobilization (Acero et al., 2006; Peretyazhko et al., 2009).

In R2–R6, the presence of OM had a major impact on metal sequestration, with high removal of all metals achieved during the first 9 months when the effluent pH was >4 (Fig. 3a–d), and a steady decrease in retention was recorded afterwards when the effluent pH was <4. In addition, under the sulfate reducing conditions found in R2–R6, divalent metals (i.e., Zn^{2+}, Cu^{2+}, Ni^{2+}, and Cd^{2+}) were predicted to precipitate as sparingly-soluble sulfides, such as ZnS, CuS, NiS_2, and CdS, or co-precipitate with Fe–S phases such as $Fe_{1+x}S$ (Walters, 2013; Barbosa et al., 2014). Moreover, newly precipitated monosulfides likely contributed to the overall higher metal remediation in bioreactors R2–R6 due to their reported ability to adsorb metals (Di Toro et al., 1992). Conversely, in the control reactor R1 which lacked an OM substrate, the sequestration was minimal for Ni, Zn, and Cd (Fig. 3a–c) and somewhat higher for Cu (Fig. 3d).

4.3. Seasonal variations

Seasonal variations in temperature, precipitation, and site-specific geochemical conditions controlled the temporal patterns of contaminant remediation in R1–R6. Seasonality also contributed to the variability in the physical and chemical parameters of the influent AMD (Figs. 1–3).

In these field experiments, temperature was the key variable, since it controlled the rate of both biological and chemical processes (Rimstidt, 2014). During the cold months (T < 10 °C), in bioreactors R2–R6, an increase of SO_4 (Fig. 2a) and decrease in H_2S (Fig. 2b) concentrations coupled with small $\Delta^{34}S_{Rx\ -IN}$ values suggests that the microbial activity at the field site diminished or even ceased, as expected (Pugh, 2013), while chemical processes proceeded at relatively lower rates. Negative $\Delta^{34}S_{R6-\ IN}$ values (Fig. 2d) suggest that partial re-oxidation of ^{32}S-rich sulfides precipitated during the fall of 2012 may have occurred during the cold months. Increasing Fe concentrations in R1–R6 effluents (Fig. 2e) was probably due to diminished FeOB activity and the subsequent precipitation of secondary solid-phases (Moncur et al., 2014). Low-temperature conditions prevailed for ~4 months, during which minimal microbial reduction of SO_4 and Fe shifted the contaminant sequestration from insoluble sulfides to pH-sensitive SO_4-rich precipitates, thus affecting the long-term stability of attenuated contaminants. During this time the AMD contaminants continued to be sequestered via chemical precipitation and sorption mechanisms within the reactors, albeit at lower reaction rates (Figs. 2 and 3). Continued precipitation of inorganic phases during the cold months, when the bacterial activity was greatly diminished, could have resulted in some coating of reactive surfaces of organic substrate matrix and limestone thus changing the environmental conditions within the bioreactors R2–R6.

The returning of warmer days (T > 10 °C) during the spring of 2013 did not lead back to the high contaminant removal efficiencies recorded in the fall of 2012 (Figs. 2 and 3). Significantly, the biochemical changes that occurred during the cold months within the bioreactors R2–R6 had a long-term impact on the system dynamics and implicitly on the remediation efficiency. Specifically, during the last eight months of the field experiments we measured a steady decline in pH (Fig. 1a) and alkalinity (Fig. 1b), moderate $\Delta^{34}S_{Rx-IN}$ values (Fig. 2d), and a steady increase in the concentrations of SO_4 (Fig. 2a), H_2S (Fig. 2b) and metal (Figs. 2 e–f, 3) in R2–R6 effluents. Changes in environmental conditions also affected the microbial community composition and the prevailing biological processes (Pugh, 2013). Most notable, microbiologic data (Fig. 4) suggest a significant decrease in sequences related to SRB during the summer and fall of 2013 as compared to fall of 2012, coinciding with the decrease in contaminant sequestration. Competition from more robust microorganisms coupled with the narrow range of optimal growth conditions of sulfate reducing-capable organisms, including lower pH values (Fig. 1a) and higher metal concentrations (Figs. 2 and 3), may have limited their re-emergence after warm weather conditions returned. Unexpectedly, $\Delta^{34}S_{Rx-IN}$ values up to 4‰ were recorded (Fig. 2d), even when the effluent was highly acidic (pH < 4), suggesting that MSR occurred within the bioreactors, but that the microorganisms responsible may have remained attached to the solid components within the individual reactors. Previous studies have also reported that the spatial organization of S-cycling is more complicated than originally predicted, with SRB differentially distributed in microenvironments (Wieringa et al., 2000; Baumgartner et al., 2006; Fike et al., 2009). Lower pH values within the bioreactors also increased the mobility of sorbed (Fulda et al., 2013; Caraballo et al., 2013) and precipitated phases (Acero et al., 2006; Borch et al., 2009; Chiriță and Schlegel, 2012; Burgos et al., 2012), thus contributing to decreased remediation efficiency.

4.4. Reactor performance based on substrate composition

Remediation of coalmine AMD occurred in all reactors R1–R6, however the presence and type of OM played a key role in the sequestration of SO_4 and metals (Fig. 6). During the 460-day experiment, the limestone-only reactor R1 retained 19 mol% SO_4, 45 mol% Fe, 36 mol% Al, 6 mol% Zn, 24 mol% Cd, and 45 mol% Cu, 2 mol% Mn, and 0.04 mol% Ni. The bioreactors (R2–R6) displayed significantly higher remediation capacity for SO_4 and most metals

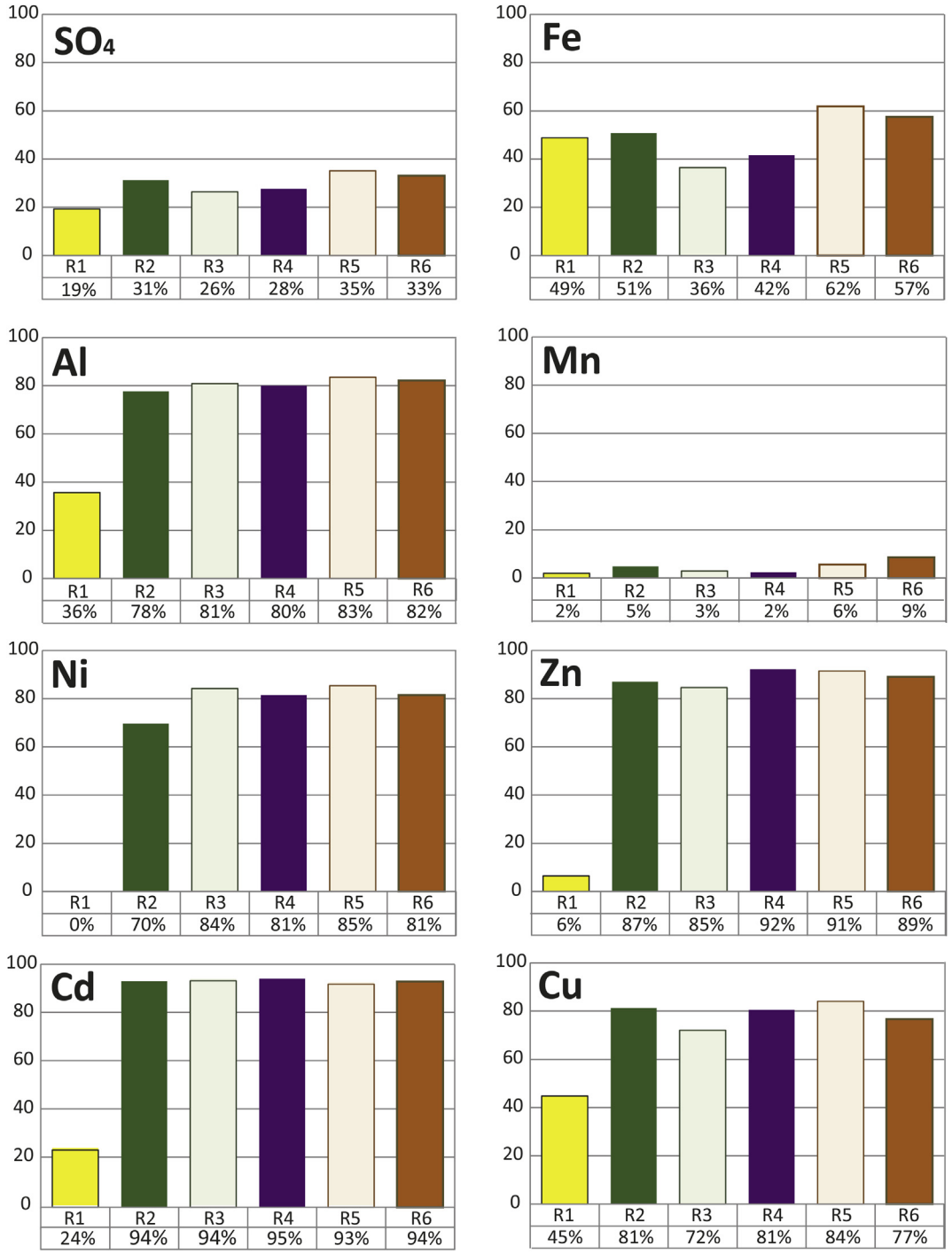

Fig. 6. Summary of remediation efficiency data expressed as contaminant percent removal (mol%) for SO_4^{2-}, Fe, Al, Mn, Ni, Zn, Cd, and Cu from the influent AMD in the control reactor R1 and organic substrate-based reactors (R2–R6) during the 460-day field experiments.

compared to that of reactor R1. Increasing the herbaceous content of the organic substrate resulted in increased removal efficiency of SO_4 from 26 to 35 mol%, Fe from 36 to 62 mol%, Al from 78 to 83 mol %, Mn from 2 to 6 mol%, Ni from 64 to 81 mol%, Zn from 88 to 95 mol %, Cu from 72 to 85 mol%, and Cd from 90 to 92 mol%.

This study shows that even if some remediation can be achieved via limestone treatment, organic substrate addition will greatly increase the sequestration of SO_4 and metals from coalmine AMD. In R2–R6, higher alkalinity produced *via* MSR processes and reduced limestone passivation have maintained relatively elevated pH values under which contaminants tend to form precipitates and sorb on surfaces, thus reducing their mobility. Previous studies have shown that the type of organic substrate and especially the amounts of cellulose and lignin and their decomposition products (Donnelly et al., 1990; Chang et al., 2000; Fioretto et al., 2005; Lee et al., 2009; Li et al., 2009; Vanholme et al., 2010) which provide simple OC for the MSR activity (Gibert et al., 2004; Pugh, 2013), controlled the efficiency of AMD treatment. The organic substrate

matrix in R2–R6 had a complex influence on remediation by (1) providing electrons for microbial reductive processes via OM degradation (Hiibel et al., 2008; Lindsay et al., 2011), (2) promoting the bioreductive precipitation of insoluble sulfides, and (3) providing active surface areas for sorption and precipitation processes (Nordstrom, 2003).). It is suggested that at the scale and within the timeframe of this field experiment lignin was a better adsorber of heavy metals than cellulose, which in turn was easier to degrade to products readily available organic carbon compounds to sulfate reducers.

The extrapolation of these results to the full-scale Tab-Simco bioreactor indicated that over the course of the 460-day period the predominantly herbaceous bioreactors (R5–R6) could remove up to 92,500 kg SO_4, 30,000 kg Fe, 8950 kg Al, and 167 kg Mn, which represents a 18.3 wt%, 36.8 wt%, 4.1 wt% and 82.3 wt% increase in SO_4, Fe, Al, and Mn, respectively, removal efficiency compared to the predominantly ligneous bioreactors (R2–R3). These results imply that aosb technologies are promising in the remediation of coal-generated AMD and increasing herbaceous content of bioreactors can enhance contaminant sequestration.

5. Conclusions and recommendations

The results of this field study demonstrate that the addition of the organic matrix layer to a limestone substrate is critical in stimulating sulfate-reducing microorganisms and therefore this approach has a good potential in remediation of the coalmine-generated AMD. Moreover, amendments that contain a large proportion of herbaceous organic substrates should predominantly be used in AOSB as reducing way of favoring the development of SRB which can lead to enhanced sequestration of SO_4, Fe, and trace metals. The limestone reactor (R1), which simulated an open limestone treatment system, sustained only a minor increase in pH and, with the exception of Fe, a lower sequestration of SO_4 and metals compared to OM-based bioreactors. However, seasonal variations in temperature are likely to adversely impact the AOSB performance over time. Specifically, the alternation of biologically-dominated processes during the warm season with abiotic-dominated processes during the cold season contributes to changes in site-specific geochemical conditions that are likely to adversely impact AOSB performance, as is shown in our study. Therefore, to enhance AOSB remediation capacity, future designs must optimize not only the organic carbon substrate but also include an AMD pretreatment phase in which the bulk of dissolved Fe/Al-species are removed from the influent AMD prior to entering the bioreactor in order to optimize the interaction between the AMD and the bioreactor substrate.

Acknowledgements

This work was supported by the Office of Surface Mining Reclamation and Enforcement (OSM) Applied Science Program Cooperative Agreement S11AC20018 AS. Mr. Paul Behum, Sr. Hydrologist, OSMRE served as the Technical Project Officer. We want to acknowledge the landowner support, Mr. and Mrs. Treg Brown of Carbondale, for granting access to the field site. The Illinois Department of Natural Resources (IDNR) assisted our team with various tasks during the duration of this study. Mr. Ron Kiser (ret.) of IDNR, Office of Mines and Minerals and Mr. Paul Behum assisted in construction of the influent collection weir structure.

The manuscript greatly benefited from constructive criticism and helpful comments by Associate Editor Michael Kersten, and three anonymous reviewers.

Appendix A. Supplementary data

Supplementary data related to this article can be found at http://dx.doi.org/10.1016/j.apgeochem.2015.08.002.

References

Acero, P., Ayora, C., Torrento, C., Nieto, J.-M., 2006. The behaviour of trace elements during schwertmannite precipitation and subsequent transformation into goethite and jarosite. Geochim. Cosmochim. Acta 70, 4130–4139.
Adams, L., Boothman, C., Lloyd, J., 2006. Identification and characterization of a novel acidotolerant Fe(III)-reducing bacterium from a 3000-year-old acidic rock drainage site. FEMS Microbiol. Lett. 268, 151–157.
Baker, B.J., Banfield, J.F., 2003. Microbial communities in acid mine drainage. FEMS Microbiol. Ecol. 44, 139–152.
Barbosa, L.P., Costa, P.F., Bertolino, S.M., Silva, J.C., Guerra-Sá, R., Leão, V.A., Teixeira, M.C., 2014. Nickel, manganese and copper removal by a mixed consortium of sulfate reducing bacteria at a high COD/sulfate ratio. World J. Microb. Biot. 30 (8), 2171–2180.
Baruah, B.P., Khare, P., 2010. Mobility of trace and potentially harmful elements in the environment from high sulphur Indian coal mines. Appl. Geochem. 25, 1621–1631.
Baumgartner, L.K., Reid, R.P., Dupraz, C., Decho, A.W., Buckley, D.H., Spear, J.R., 2006. Sulfate reducing bacteria in microbial mats: changing paradigms, new discoveries. Sediment. Geol. 185, 131–145.
Becerra, C.A., Lopez-Luna, E.L., Ergas, S.J., Nusslein, K., 2009. Microcosm-based study of the attenuation of an acid mine drainage-impacted site through biological sulfate and iron reduction. Geomicrobiol. J. 26, 9–20.
Behum, P.T., Lefticariu, L., Bender, K.S., Segid, Y.T., Burns, A.S., Pugh, C.W., 2011. Remediation of coal-mine drainage by a sulfate-reducing bioreactor: a case study from the Illinois coal basin, USA. Appl. Geochem. 26, S162–S166.
Bertis, V.J., Ziebis, W., 2010. Bioturbation and the role of microniches for sulfate reduction in coastal marine sediments. Environ. Microbiol. 12, 3022–3034.
Bigham, J.M., Nordstrom, D.K., 2000. Iron and aluminum hydroxysulfates from acid sulfate waters. Rev. Mineral. Geochem. 40 (1), 351–403.
Blowes, D.W., Ptacek, C.J., Jambor, J.L., Weisener, C.G., Paktunc, D., Gould, W.D., Johnson, D.B., 2014. The geochemistry of acid mine drainage. In: Sherwood Lollar, B. (Ed.), Environmental Geochemistry. Holland, H.D., Turekian, K.K. (Exec. Eds.), Treatise on Geochemistry, vol. 11. Elsevier, pp. 113–190.
Borch, T., Kretzschmar, R., Kappler, A., Cappellen, P.V., Ginder-Vogel, M., Voegelin, A., Campbell, K., 2009. Biogeochemical redox processes and their impact on contaminant dynamics. Environ. Sci. Technol. 44, 15–23.
Brown Jr., G.E., Parks, G.A., 2001. Sorption of trace elements on mineral surfaces: modern perspectives from spectroscopic studies, and comments on sorption in the marine environment. Intl. Geol. Rev. 43, 963–1073.
Burgos, W.D., Borch, T., Troyer, L., Luan, F., Larson, L., Brown, J.F., Shimizu, M., 2012. Schwertmannite and Fe oxides formed by biological low-pH Fe (II) oxidation versus abiotic neutralization: impact on trace metal sequestration. Geochim. Cosmochim. Acta 76, 29–44.
Burns, A.S., Pugh, C.W., Segid, Y.T., Behum, P.T., Lefticariu, L., Bender, K.S., 2012. Performance and microbial community dynamics of a sulfate-reducing bioreactor treating coal generated acid mine drainage. Biodegradation 23 (3), 415–429.
Campbell, L.L., Postgate, J.R., 1965. Classification of the spore-forming sulfate-reducing bacteria. Bacteriol. Rev. 29 (3), 359.
Canfield, D.E., 2001. Biogeochemistry of sulfur isotopes. Stable Isot. Geochem. Rev. Mineral. Geochem. 43, 607–636.
Caporaso, J.G., Kuczynski, J., Stombaugh, J., Bittinger, K., Bushman, F.D., Costello, E.K., Fierer, N., Pena, A.G., Goodrich, J.K., Gordon, J.I., Huttley, G.A., Kelley, S.T., Knights, D., Koenig, J.E., Ley, R.E., Lozupone, C.A., McDonald, D., Muegge, D.B., Pirrung, M., Reeder, J., Sevinsky, J.R., Turnbaugh, P.J., Walters, W.A., Widmann, J., Yatsunenko, T., Zaneveld, J., Knight, R., 2010. QIIME allows analysis of high-throughput community sequencing data. Nat. Methods 7, 335–336.
Caraballo, M.A., Rimstidt, J.D., Macías, F., Nieto, J.M., Hochella Jr., M.F., 2013. Metastability, nanocrystallinity and pseudo-solid solution effects on the understanding of schwertmannite solubility. Chem. Geol. 360–361, 22–31.
Chang, I.S., Shin, P.K., Kim, B.H., 2000. Biological treatment of acid mine drainage under sulphate-reducing conditions with solid waste materials as substrate. Water Res. 34 (4), 1269–1277.
Chen, M., Guining, L., Chuling, G., Chengfang, Y., Jingxiong, W., Weilin, H., Nathan, Y., Zhi, D., 2015. Sulfate migration in a river affected by acid mine drainage from the Dabaoshan mining area, South China. Chemosphere 119, 734–743.
Chiriţă, P., Schlegel, M.L., 2012. Reaction of FeS with Fe (III)-bearing acidic solutions. Chem. Geol. 334, 131–138.
Cocos, I., Zagury, G.J., Clément, B., Samson, R., 2002. Multiple factor design for reactive mixture selection for use in reactive walls in mine drainage treatment. Water Res. 36 (1), 167–177.
Coggon, M., Becerra, C.A., Nüsslein, K., Miller, K., Yuretich, R., Ergas, S.J., 2012. Bioavailability of jarosite for stimulating acid mine drainage attenuation. Geochim. Cosmochim. Acta 78, 65–76.
Cornell, R.M., Schwertmann, U., 2003. The Iron Oxides: Structure, Properties, Reactions, Occurrence and Uses, second ed. Wiley VCH Publishers, New York, p. 703.

Cravotta III, C.A., 2008. Dissolved metals and associated constituents in abandoned coal-mine discharges, Pennsylvania, USA. Part 1: constituent concentrations and correlations. Appl. Geochem. 23, 166–202.
Cravotta III, C.A., Trahan, M.K., 1999. Limestone drains to increase pH and remove dissolved metals from acidic mine drainage. Appl. Geochem. 14, 581–606.
Davranche, M., Dia, A., Fakih, M., Nowack, B., Gruau, G., Ona-nguema, G., Hochreutener, R., 2013. Organic matter control on the reactivity of Fe (III)-oxyhydroxides and associated as in wetland soils: a kinetic modeling study. Chem. Geol. 335, 24–35.
Desai, M.S., Assig, K., Dattagupta, S., 2013. Nitrogen fixation in distinct microbial niches within a chemoautotrophy-driven cave ecosystem. ISME J. 7, 2411–2423.
Di Toro, D.M., Mahony, J.D., Hansen, D.J., Scott, K.J., Carlson, A.R., Ankley, G.T., 1992. Acid volatile sulfide predicts the acute toxicity of cadmium and nickel in sediments. Environ. Sci. Technol. 26, 96–101.
Donnelly, P.K., Entry, J.A., Crawford, D.L., Cromack Jr., K., 1990. Cellulose and lignin degradation in forest soils: response to moisture, temperature, and acidity. Microb. Ecol. 20 (1), 289–295.
Druschel, G.K., Baker, B.J., Gihring, T.M., Banfield, J.F., 2004. Acid mine drainage biogeochemistry at Iron Mountain, California. Geochem. Trans. 5 (2), 13–32.
España, J.S., Pamo, E.L., Pastor, E.S., Andrés, J.R., Rubí, J.M., 2006. The removal of dissolved metals by hydroxysulphate precipitates during oxidation and neutralization of acid mine waters, Iberian Pyrite Belt. Aqua. Geochem. 12 (3), 269–298.
Fike, D.A., Finke, N., Zha, J., Blake, G., Hoehler, T.M., Orphan, V.J., 2009. The effect of sulfate concentration on (sub)millimeter-scale sulfide $\delta^{34}S$ in hypersaline cyanobacterial mats over the diel cycle. Geochim. Cosmochim. Acta 73, 6187–6204.
Fioretto, A., Di Nardo, C., Papa, S., Fuggi, A., 2005. Lignin and cellulose degradation and nitrogen dynamics during decomposition of three leaf litter species in a Mediterranean ecosystem. Soil Biol. Biochem. 37 (6), 1083–1091.
Fulda, B., Voegelin, A., Kretzschmar, R., 2013. Redox-controlled changes in cadmium solubility and solid-phase speciation in a paddy soil as affected by reducible sulfate and copper. Environ. Sci. Technol. 47 (22), 12775–12783.
Gagliano, W.B., Brill, M.R., Bigham, J.M., Jones, F.S., Traina, S.J., 2004. Chemistry and mineralogy of ochreous sediments in a constructed mine drainage wetland. Geochim. Cosmochim. Acta 68, 2119–2128.
Gerth, J., 1990. Unit-cell dimensions of pure and trace metal- associated goethites. Geochim. Cosmochim. Acta 54, 363–371.
Gibert, O., De Pablo, J., Cortina, J.L., Ayora, C., 2004. Chemical characterisation of natural organic substrates for biological mitigation of acid mine drainage. Water Res. 38 (19), 4186–4196.
Glombitza, F., 2001. Treatment of acid lignite mine flooding water by means of microbial sulfate reduction. Waste Manag. 21 (2), 197–203.
Greben, H.A., Maree, J.P., Singmin, Y., Mnqanqeni, S., 2000. Biological sulphate removal from acid mine effluent using ethanol as carbon and energy source. Water Sci. Technol. 42 (3–4), 339–344.
Guo, X., Zhang, S., Shan, X.Q., 2008. Adsorption of metal ions on lignin. J. Hazard. Mater. 151, 134–142.
Hammarstrom, J.M., Seal II, R.R., Meier, A.L., Kornfeld, J.M., 2005. Secondary sulfate minerals associated with acid drainage in the eastern US: recycling of metals and acidity in surficial environments. Chem. Geol. 215, 407–431.
Hansel, C.M., Benner, S.G., Neiss, J., Dohnalkova, A., Kukkadapu, R.K., Fendorf, S., 2003. Secondary mineralization pathways induced by dissimilatory iron reduction of ferrihydrite under advective flow. Geochim. Cosmochim. Acta 67, 2977–2992.
Harris, M., Ragusa, S., 2001. Bioremediation of acid mine drainage using decomposable plant material in a constant flow bioreactor. Environ. Geol. 40 (10), 1192–1204.
Hedin, R.S., 1989. Treatment of coal mine drainage with constructed wetlands. In: Majumdar, S.K., Brooks, R.P., Brenner, F.J., Tiner, R.W. (Eds.), Wetlands Ecology and Conservation: Emphasis in Pennsylvania. The Pennsylvania Academy of Science, pp. 349–362.
Hedin, R.S., Watzlaf, G.R., Nairn, R.W., 1994. Passive treatment of acid mine drainage with limestone. J. Environ. Qual. 23, 1338–1345.
Hedrich, S., Schlömann, M., Johnson, D.B., 2011. The iron-oxidizing proteobacteria. Microbiology 157, 1551–1564.
Hiibel, S.R., Pereyra, L.P., Inman, L.Y., Tischer, A., Reisman, D.J., Reardon, K.F., Pruden, A., 2008. Microbial community analysis of two field-scale sulfate-reducing bioreactors treating mine drainage. Environ. Microbiol. 10 (8), 2087–2097.
Huminicki, D.M., Rimstidt, J.D., 2008. Neutralization of sulfuric acid solutions by calcite dissolution and the application to anoxic limestone drain design. Appl. Geochem. 23 (2), 148–165.
Johnson, D.B., Hallberg, K.B., 2005. Acid mine drainage remediation options: a review. Sci. Total Environ. 338 (1–2), 3–14.
Johnson, D.B., Kanao, T., Hedrich, S., 2012. Redox transformation of iron at extremely low pH: fundamental and applied aspects. Front. Microbiol. 3, 96.
Jolivet, J.P., Chanéac, C., Tronc, E., 2004. Iron oxide chemistry. From molecular clusters to extended solid networks. Chem. Commun. 5, 481–483.
Komilis, D.P., Ham, R.K., 2003. The effect of lignin and sugars to the aerobic decomposition of solid wastes. Waste Manag. 23 (5), 419–423.
Koschorreck, M., 2008. Microbial sulphate reduction at a low pH. FEMS Microbiol. Ecol. 64, 329–342.
Koschorreck, M., Frömmichen, R., Herzsprung, P., Tittel, J., Wendt-Potthoff, K., 2002. Functions of straw for in situ remediation of acidic mining lakes. Water, Air Soil Pollut. Focus 2 (3), 97–109.
Lee, G., Bigham, J.M., Faure, G., 2002. Removal of trace metals by co-precipitation with Fe, Al and Mn from natural waters contaminated with acid mine drainage in the Ducktown Mining District, Tennessee. Appl. Geochem. 17 (5), 569–581.
Lee, S.H., Doherty, T.V., Linhardt, R.J., Dordick, J.S., 2009. Ionic liquid-mediated selective extraction of lignin from wood leading to enhanced enzymatic cellulose hydrolysis. Biotechnol. Bioeng. 102 (5), 1368–1376.
Lefticariu, L., Pratt, L.M., Ripley, E.M., 2006. Mineralogic and sulfur isotopic effects accompanying oxidation of pyrite in millimolar solutions of hydrogen peroxide at temperatures from 4 to 150°C. Geochim. Cosmochim. Acta 70 (19), 4889–4905.
Lentini, C.L., Wankel, S.D., Hansel, C.M., 2012. Enriched iron(III)-reducing bacterial communities are shaped by carbon substrate and iron oxide mineralogy. Front. Microb. Chem. 3 (404), 1–19.
Li, J., Yuan, H., Yang, J., 2009. Bacteria and lignin degradation. Front. Biol. China 4 (1), 29–38.
Lindsay, M.B.J., Blowes, D.W., Condon, P.D., Ptacek, C.J., 2011. Organic carbon amendments for passive in situ treatment of mine drainage: field experiments. Appl. Geochem. 26, 1169–1183.
Luan, F., Santelli, C.M., Hansel, C.M., Burgos, W.D., 2012. Defining manganese(II) removal processes in passive coal mine drainage treatment systems through laboratory incubation experiments. Appl. Geochem. 27 (8), 1567–1578.
Majzlan, J., Myneni, S.C.B., 2004. Speciation of iron and sulfate in acid waters: aqueous clusters to mineral precipitates. Environ. Sci. Technol. 39 (1), 188–194.
Meier, J., Piva, A., Fortin, D., 2012. Enrichment of sulfate-reducing bacteria and resulting mineral formation in media mimicking pore water metal ion concentrations and pH conditions of acidic pit lakes. FEMS Microbiol. Ecol. 79, 69–84.
Merdy, P., Guillon, E., Aplincourt, M., 2002. Iron and manganese surface complex formation with extracted lignin. Part 1: adsorption isotherm experiments and EPR spectroscopy analysis. New J. Chem. 26 (11), 1638–1645.
Meyer, B., Kuever, J., 2007. Phylogeny of the alpha and beta subunits of the dissimilatory adenosine-5′-phosphosulfate (APS) reductase from sulfate-reducing prokaryotes–origin and evolution of the dissimilatory sulfate-reduction pathway. Microbiol. 153 (7), 2026–2044.
Moncur, M.C., Ptacek, C.J., Hayashi, M., Blowes, D.W., Birks, S.J., 2014. Seasonal cycling and mass-loading of dissolved metals and sulfate discharging from an abandoned mine site in northern Canada. Appl. Geochem. 41, 176–188.
Moreau, J.W., Zierenberg, R.A., Banfield, J.F., 2010. Diversity of dissimilatory sulfite reductase genes (dsrAB) in a salt marsh impacted by long-term acid mine drainage. Appl. Environ. Microbiol. 76, 4819–4828.
Nancucheo, I., Johnson, D.B., 2012. Selective removal of transition metals from acidic mine waters by novel consortia of acidophilic sulfidogenic bacteria. Microb. Biotechnol. 5, 34–44.
Neculita, C.M., Zagury, G.J., Bussière, B., 2007. Passive treatment of acid mine drainage in bioreactors using sulfate-reducing bacteria: critical review and research needs. J. Environ. Qual. 36, 1–16.
Neculita, C.M., Yim, G.J., Lee, G., Ji, S.W., Jung, J.W., Park, H.S., Song, H., 2011. Comparative effectiveness of mixed organic substrates to mushroom compost for treatment of mine drainage in passive bioreactors. Chemosphere 83, 76–82.
Newcombe, C.E., Brennan, R.A., 2009. Improved passive treatment of acid mine drainage in mushroom compost amended with crab-shell chitin. J. Environ. Eng. 136 (6), 616–626.
Nordstrom, D.K., 2003. Effects of microbiological and geochemical interactions in mine drainage. In: Jambor, J.L., Blowes, D.W., Ritchie, A.I.M. (Eds.), Environmental Aspects of Mine Wastes, Short Course Series, vol. 31. Mineralogical Association of Canada, Ottawa, Ontario, Canada, pp. 227–238.
Nordstrom, D.K., 2011. Hydrogeochemical processes governing the origin, transport and fate of major and trace elements from mine wastes and mineralized rock to surface waters. Appl. Geochem. 26, 1777–1791.
Palmer, M.A., Bernhardt, E.S., Schlesinger, W.H., Eshleman, K.N., Foufoula-Georgiou, E., Hendryx, M.S., Lemly, A.D., Likens, G.E., Loucks, O.L., Power, M.E., White, P.S., Wilcock, P.R., 2010. Mountaintop mining consequences. Science 327, 148–149.
Peretyazhko, T., Zachara, J.M., Boily, J.F., Xia, Y., Gassman, P.L., Arey, B.W., Burgos, W.D., 2009. Mineralogical transformations controlling acid mine drainage chemistry. Chem. Geol. 262 (3), 169–178.
Pérez, J., Munoz-Dorado, J., de la Rubia, T.D.L.R., Martinez, J., 2002. Biodegradation and biological treatments of cellulose, hemicellulose and lignin: an overview. Int. Microbiol. 5 (2), 53–63.
Pérez, N.A., Rincón, G., Delgado, L.A., González, N., 2006. Use of biopolymers for the removal of heavy metals produced by the oil industry—A feasibility study. Adsorption 12 (4), 279–286.
Praharaj, T., Fortin, D., 2004. Indicators of microbial sulfate reduction in acidic sulfide-rich mine tailings. Geomicrob. J. 21, 457–467.
Pruden, A., Messner, N., Pereyra, L., Hanson, R.E., Hiibel, S.R., Reardon, K.F., 2007. The effect of inoculum on the performance of sulfate-reducing columns treating heavy metal contaminated water. Water Res. 41 (4), 904–914.
Pugh, C.W., 2013. Effect of Substrate Composition on Metabolic Diversity and Efficiency of in Situ Pilot Scale Passive Sulfate-reducing Bioreactors Treating Acid Mine Drainage. M.S. thesis. Southern Illinois University.
Quintana, G.C., Rocha, G.J., Gonçalves, A.R., Velásquez, J.A., 2008. Evaluation of heavy metal removal by oxidised lignins in acid media from various sources. BioResources 3 (4), 1092–1102.
Rabus, R., Hansen, T.A., Widded, F., 2013. Dissimilatory sulfate- and sulfur-reducing

prokaryotes. In: Rosenberg, E. (Ed.), The Prokaryotes – Prokaryotic Physiology and Biochemistry. Springer-Verlag, Berlin Heidelberg, pp. 309–404.
Reddad, Z., Gerente, C., Andres, Y., Le Cloirec, P., 2002. Adsorption of several metal ions onto a low-cost biosorbent: kinetic and equilibrium studies. Environ. Sci. Technol. 36 (9), 2067–2073.
Rimstidt, D., 2014. Geochemical Rate Models: an Introduction to Geochemical Kinetics. Cambridge University Press, 239 pp.
Robinson-Lora, M.A., Brennan, R., 2010. Chitin complex for the remediation of mine impacted water: geochemistry of metal removal and comparison with other common substrates. Appl. Geochem. 25 (3), 336–344.
Rose, S., Ghazi, A.M., 1997. Release of sorbed sulfate from iron oxyhydroxides precipitated from acid mine drainage associated with coal mining. Environ. Sci. Technol. 31 (7), 2136–2140.
Sallam, A., Steinbüchel, A., 2009. *Clostridium sulfidigenes* sp. nov., a mesophilic, proteolytic, thiosulfate-and sulfur-reducing bacterium isolated from pond sediment. Int. J. Syst. Evol. Microbiol. 59 (7), 1661–1665.
Sánchez-Andrea, I., Sanz, J.L., Bijmans, M.F., Stams, A.J., 2014. Sulfate reduction at low pH to remediate acid mine drainage. J. Hazard Mater. 269, 98–109.
Santelli, C.M., Pfister, D., Lazarus, D., Sun, L., Burgos, W., Hansel, C., 2010. Promotion of Mn (II) oxidation and remediation of coal mine drainage in passive treatment systems by diverse fungal and bacterial communities. Appl. Environ. Microbiol. 76 (14), 4871–4875.
Senko, J.M., Wanjugi, P., Lucas, M., Bruns, M.A., Burgos, W.D., 2008. Characterization of Fe(II) oxidizing bacterial activities and communities at two acidic Appalachian coalmine drainage-impacted sites. ISME J. 2, 1134–1145.
Senko, J.M., Zhang, G.X., McDonough, J.T., Bruns, M.A., Burgos, W.D., 2009. Metal reduction at low pH by a desulfosporosinus species: implications for the biological treatment of acidic mine drainage. Geomicrobiol. J. 26, 71–82.
Stumm, W., Morgan, K., 1996. Aquatic Chemistry, third ed. Wiley-Interscience, New York, NY.
Sun, L., Pope, P.B., Eijsink, V.G.H., Schnürer, A., 2015. Characterization of microbial community structure during continuous anaerobic digestion of straw and cow manure. Microb. Biotechnol. http://dx.doi.org/10.1111/1751-7915.12298.
Swedlund, P.J., Webster, J.G., Miskelly, G.M., 2009. Goethite adsorption of Cu (II), Pb (II), Cd (II), and Zn (II) in the presence of sulfate: properties of the ternary complex. Geochim. Cosmochim. Acta 73 (6), 1548–1562.
Thirumavalavan, M., Lai, Y.L., Lin, L.C., Lee, J.F., 2009. Cellulose-based native and surface modified fruit peels for the adsorption of heavy metal ions from aqueous solution: Langmuir adsorption isotherms. J. Chem. Eng. Data 55 (3), 1186–1192.
Vanholme, R., Demedts, B., Morreel, K., Ralph, J., Boerjan, W., 2010. Lignin biosynthesis and structure. Plant Physiol. 153 (3), 895–905.
Walters, E.R., 2013. Sulfate Reducing Bioreactor Dependence on Organic Substrates for Long-term Remediation of Acid Mine Drainage: Field Experiments. M.S. Thesis. Southern Illinois University.
Wang, W., Zhang, X., Wang, H., Wang, X., Zhou, L., Liu, R., Liang, Y., 2012. Laboratory study on the adsorption of Mn^{2+} on suspended and deposited amorphous $Al(OH)_3$ in drinking water distribution systems. Water Res. 46 (13), 4063–4070.
Wieringa, E.B.A., Overmann, J., Cypionka, H., 2000. Detection of abundant sulphate-reducing bacteria in marine oxic sediment layers by a combined cultivation and molecular approach. Environ. Microbiol. 2, 417–427.
Wirth, R., Kovács, E., Maróti, G., Bagi, Z., Rákhely, G., Kovács, K.L., 2012. Characterization of a biogas-producing microbial community by short-read next generation DNA sequencing. Biotechnol. Biofuels 5 (1), 41.
Zachara, J.M., Kukkadapu, R.K., Fredrickson, J.K., Gorby, Y.A., Smith, S.C., 2002. Biomineralization of poorly crystalline Fe(III) oxides by dissimilatory metal reducing bacteria (DMRB). Geomicrobiol. J. 19, 179–207.
Zagury, G.J., Kulnieks, V.I., Neculita, C.M., 2006. Characterization and reactivity assessment of organic substrates for sulphate-reducing bacteria in acid mine drainage treatment. Chemosphere 64, 944–954.
Ziegler, S., Dolch, K., Geiger, K., Krause, S., Asskamp, M., Esterhues, K., Kriews, M., Wilhelms-Dick, D., Goettlicher, J., Majzlan, J., Gescher, J., 2013. Oxygen-dependent niche formation of a pyrite-dependent acidophilic consortium built by archaea and bacteria. ISME J. 7, 1725–1737.